

Effect of martensite on cold cracking in 600-MPa grade flux-cored arc weld metals using the Y-groove test

Myungjin Lee¹ · Kyungmok Cho¹ · Yongdeok Kim² · Namhyun Kang¹

Received: 4 September 2014 / Accepted: 4 March 2015 / Published online: 21 March 2015
© International Institute of Welding 2015

Abstract This study observed the cold crack susceptibility of three types of low-hydrogen flux-cored arc (FCA)-weld metals developed for a yield strength of 600 MPa. Cold cracks in the weld metal were measured using the Y-groove test, and four different preheating temperatures were employed from room temperature to 150 °C. The microstructure of the Y-groove weldment consisted of acicular ferrite, bainite, and martensite. All weld metals showed cold cracking at room temperature, and a preheating temperature of 50 °C produced cold cracking only for weld metal C, having the largest carbon equivalent and the largest volume fraction of bainite and martensite. The volume expansion ratio of the weld metals was measured when the austenite was transformed to martensite during simulated weld cooling. Weld metal C showed the largest volume expansion ratio (2.6 %), resulting in the largest probability of cold crack production. Moreover, the martensite affected the cold crack fractography in the weld metal. Intergranular fracture occurred in the region occupied by large volume fractions of martensite, and quasi-cleavage fracture was observed in regions of small-volume fractions of martensite. Large amounts of martensite were related to the regions of high Mn content and corresponding to intergranular fracture.

Keywords (IIW Thesaurus) FCA welding · Cold cracking · Preheating · Martensite · Segregation · Ferrite

Doc. IIW-2552, recommended for publication by Commission II “Arc Welding and Filler Metals”.

✉ Namhyun Kang
nhkang@pusan.ac.kr

¹ Department of Materials Science and Engineering, Pusan National University, Busan 609-735, South Korea

² Research and Development Center, Hyundai Welding Co., Ltd, Pohang 790-240, South Korea

1 Introduction

Owing to increasing energy consumption, new oil and natural gas resources need to be excavated, and new ocean plants are required to be built. As the scale of offshore facilities becomes increasingly massive, the strength of steels used in these ocean plants must also increase. To acquire high strength, steel for the ocean plants is prepared by applying various alloying elements and heat treatment processes [1, 2]. As a part of this process, the carbon equivalent (Ceq) content of high-strength steels is increased, which promotes cold cracking after welding. To minimise cold cracking with increasing strength, preheating and/or post-heating processes need to be applied for welding, even though the processes decrease weld productivity. When advanced high-strength steels are developed, the weld consumable needs to match the mechanical properties of the base metal. Steel plates for the ocean plants are normally welded by using flux-cored arc (FCA) to maximise weld productivity [3]. However, FCA-weld metals are more sensitive to cold cracking compared to solid wire because of their large moisture adsorption [4, 5].

Cold cracking is frequently observed at heat-affected zone (HAZ) and weld metal at temperatures below 200 °C. The factors contributing to cold cracks are diffusible hydrogen, tensile residual stress and a susceptible microstructure in the weld metal [6–8]. As the steel strength increases, the occurrence of cold cracking in the weld metal also increases [9]. In case of the FCA welding, welding parameters significantly affect the diffusible hydrogen in the weld metal, and many studies have investigated the effect of welding parameters and diffusible hydrogen on cold cracking in weld metals [10–16]. Furthermore, in order to suppress the occurrence of cold cracking in weld metals, many studies have been conducted to reduce the diffusible hydrogen in FCA-weld wires [17–19]. Hart et al. reported that the effect of microstructure

was greater than that of diffusible hydrogen on cold cracking in weldment when the content of diffusible hydrogen was less than 5 ml/100 g [20]. However, the reduction of diffusible hydrogen has a limit when using metal powder because the effect of flux dominates the absorption of hydrogen. As a result of this limit, the study of microstructural effects on cold cracking in FCA weld metal has increased in recent times [21–23]. There are various microstructures in the weld metal, with grain boundary ferrite and acicular ferrite being the dominant microstructures for weldments having a yield strength of less than 600 MPa. The relationship between ferrite and cold crack sensitivity has been previously studied [22, 23]; however, there are few studies on the effect of martensite on the cold cracking of weld metals, which is known to be significantly sensitive to cold cracking.

The objective of the study is to investigate, with the Y-groove test, cold crack behaviour in low-hydrogen FCA-weld metals having a yield strength of 600 MPa. Weld metal composition and preheating temperature were varied to study the effect of microstructure on the cold crack ratio. Furthermore, cold crack fractography and volume expansion ratio during the martensite transformation were correlated to the microstructure for understanding cold crack behaviour.

2 Experimental procedure

Table 1 shows the chemical composition, diffusible hydrogen content and mechanical properties of three types of low-hydrogen FCA-weld metals having a yield strength of 600 MPa. The chemical composition of the weld metals was analysed by optical emission spectroscopy, and the carbon equivalent was calculated using the formula recommended by the International Institute of Welding (IIW) [24]. The content of diffusible hydrogen (HD) in the weldment was measured by gas chromatography [25].

The weld metals A to C had various C_{eq} values from 0.37 to 0.48, and the same level of HD. The weld metals A to C showed a change in yield/tensile strengths and elongation with respect to C_{eq} .

A cold crack experiment was conducted using the Y-groove test according to the ISO standard [26]. Thick EH36

plates of 50 mm were used as the base metal for the Y-groove test. The groove shape was changed in this study to a capital ‘Y’, as indicated in Fig. 1, to simulate a weld joint in real applications. The Y-groove weldments were cut into five sections to measure the cold crack ratio by optical microscopy [27]. The welding voltage and currents to produce the Y-groove specimens were 27 V and 240 A, respectively. The welding speed was 50 cm/min and the heat input for welding was 0.7 kJ/mm. One hundred percent CO₂ was used as a shielding gas. Various preheating temperatures were employed during the Y-groove test: room temperature, 50, 100 and 150 °C.

The Y-groove weld specimens were etched with 2 % nital solution, and the microstructure was analysed by optical microscopy and scanning electron microscopy. The cold crack cross-sections were examined using scanning electron microscopy and electron back-scatter diffraction (EBSD). Because of the fine grain size in the weldments, the microstructure volume fractions were measured using EBSD IQ 7 maps at $\times 3000$ magnification and characterised by image analysis (i Solution DT). The study identified bainite and martensite phases as compared to acicular ferrite by colour and shape of the grain. Bainite and martensite were categorised by dark gray and fine lath shape. Acicular ferrite was delineated by light gray and thin lenticular/plate shape. The dilatometer test specimens were taken from the Y-groove weld specimens to measure the volume expansion ratio. The dilatometer specimens had a cylindrical rod shape and were 4 mm in diameter and 10 mm long. The dilatometer test was conducted under the following conditions: heated to 1000 °C, held for 1 min and cooled down to room temperature with a cooling rate 60 °C/s. In order to find the influence of segregation on cold cracking, electron probe micro-analysis (EPMA) was conducted in the cold crack cross-section.

3 Results and discussion

3.1 Effect of preheat temperature and weld composition on Y-groove weld microstructures

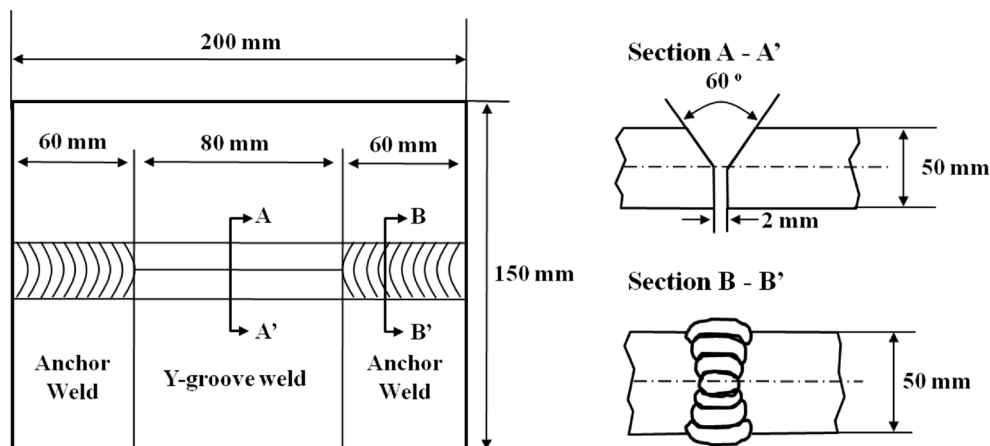
The multi-pass weldment of 600-MPa grade was decorated with grain boundary ferrite, Widmännstätten ferrite and acicular

Table 1 Chemical composition and mechanical properties of weld metals

No	C	Si	Mn	Ni	Ti	Al+Nb+V+B	C_{eq}^a	HD (ml/100 g)	Yield strength (MPa)	Tensile strength (MPa)	Elongation (%)
A	0.053	0.29	1.19	1.59	0.030	0.052	0.37	4.05	551	583	28.2
B	0.062	0.22	1.19	2.06	0.041	0.033	0.41	4.15	632	644	24.4
C	0.059	0.42	1.44	2.55	0.058	0.032	0.48	4.39	675	695	23.4

^a $C_{eq}(IIW) = C + \frac{Mn}{6} + \frac{Cr+Mo+V}{5} + \frac{Ni+Cu}{15}$

Fig. 1 Schematic illustration of Y-groove weld cracking test



ferrite [28, 29]. However, the Y-groove test was produced with one pass welding, therefore inducing rapid cooling and no tempering due to subsequent welding passes, as compared with the case of multi-pass welding. For this reason, the microstructure of Y-groove weld metal consisted of acicular ferrite, bainite and martensite. Figure 2 shows the volume fraction of acicular ferrite, bainite and martensite in the weld metal as a function of preheat temperature and weld metal composition. With no preheating, the volume fraction of acicular ferrite was 41, 46 and 29 % for specimens A, B and C, respectively. Specimen C, having the largest C_{eq} (0.48), produced bainite and martensite volume fractions in excess of 70 %; however, specimens A and B had a small C_{eq} (0.37 and 0.41), resulting in the production of only a small amount of bainite and martensite. Large amounts of alloying elements in specimen C increased the hardenability, therefore producing a large amount of bainite and martensite. The C_{eq} of B specimen (0.41) was approximately the same as that of specimen A (0.37), therefore producing approximately the same volume fraction of acicular ferrite as each other. As the preheat temperature increased to 150 °C, the volume fraction of martensite and bainite decreased and the volume fraction of acicular

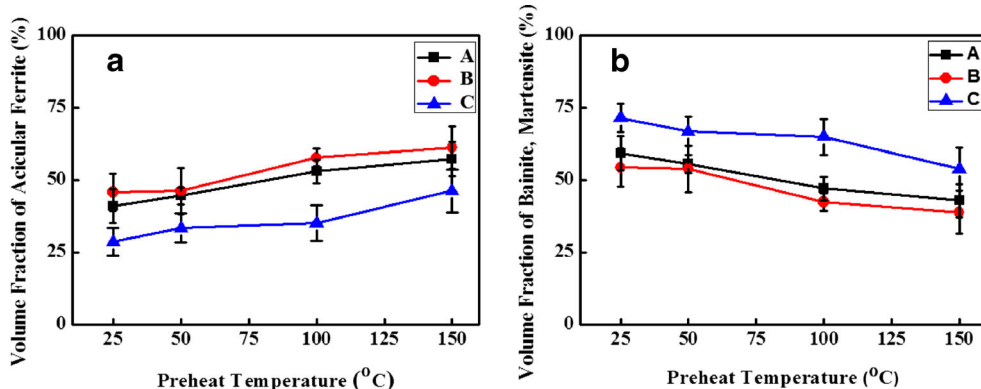
ferrite increased, as shown in Fig. 2, because the cooling rate decreased as the preheating temperature increased.

3.2 Effect of preheat temperature and weld composition on cold crack ratio

Figure 3 indicates the effect of preheat temperature and weld metal composition on the cold crack ratio. All Y-groove specimens A to C showed cold cracking in the weld metal at room temperature. A preheating temperature of 50 °C produced a cold crack in specimen C, but no cold cracks for specimens A and B. The cold crack phenomenon disappeared as the preheating temperature increased to 100 and 150 °C for all specimens A to C. Only specimen C, having the largest C_{eq} (0.48), showed a cold crack at a preheat temperature of 50 °C. Furthermore, specimen C had the largest cold crack ratio at room temperature.

Fractographs taken after the Y-groove test, shown in Fig. 4, confirm the cold crack behaviour. Cold crack fractographs showed a combination of intergranular fracture and quasi-cleavage fracture. Intergranular fracture

Fig. 2 Volume fractions of weld microstructure as a function of preheat temperature and weld metal composition: **a** acicular ferrite and **b** a mixture of bainite and martensite



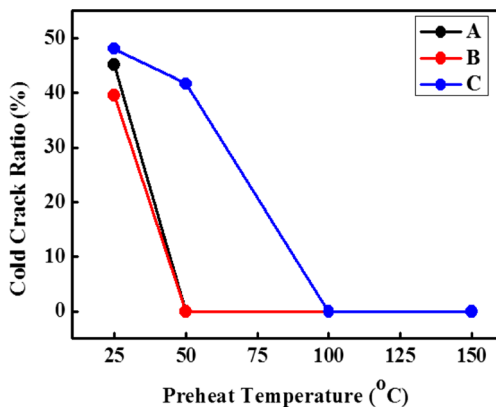
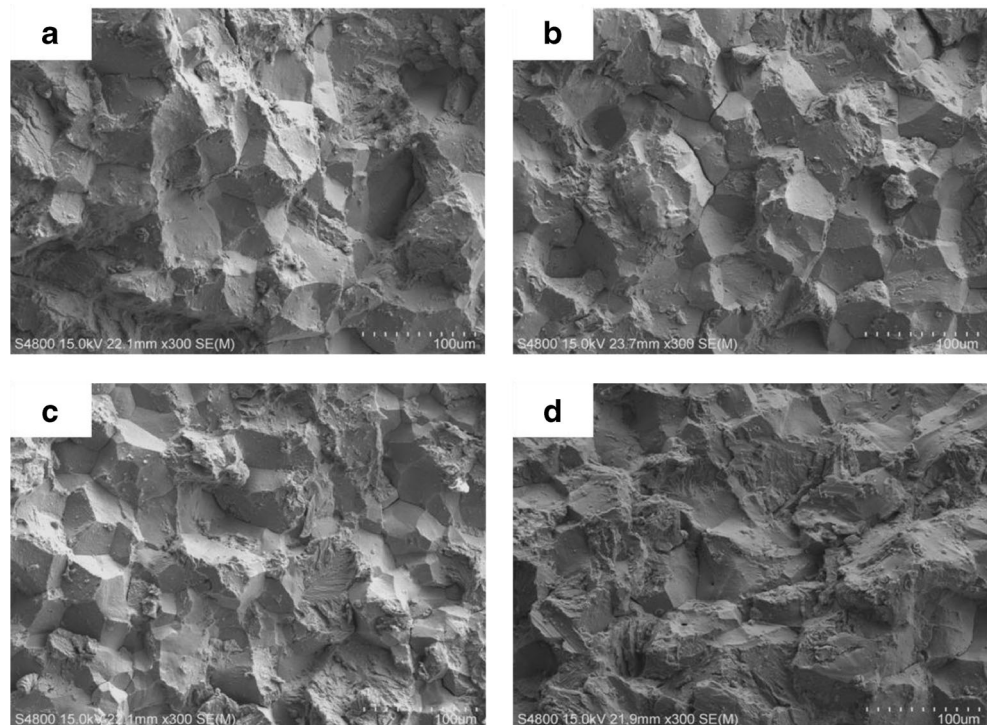


Fig. 3 Cold crack ratio as a function of the weld metal and preheating temperature

had a flat failure plane, and quasi-cleavage fracture showed some rough and ductile planes. The fracture surface of weld metals at room temperature indicated mainly intergranular fracture, regardless of the welding metal type, as depicted in Fig. 4a–c. As the preheating temperature increased to 50 °C, the quasi-cleavage fractures appeared, as shown in Fig. 4d, which is probably due to the decrease in the bainite and martensite volume fractions as the preheating temperature increased to 50 °C. Specimen C, having the largest C_{eq} , had the largest amount of bainite and martensite, therefore producing the largest amount of cold cracking.

Fig. 4 Cold crack fractographs of weld metals: **a** specimen A at room temperature, **b** specimen B at room temperature, **c** specimen C at room temperature and **d** specimen C at a preheat temperature 50 °C

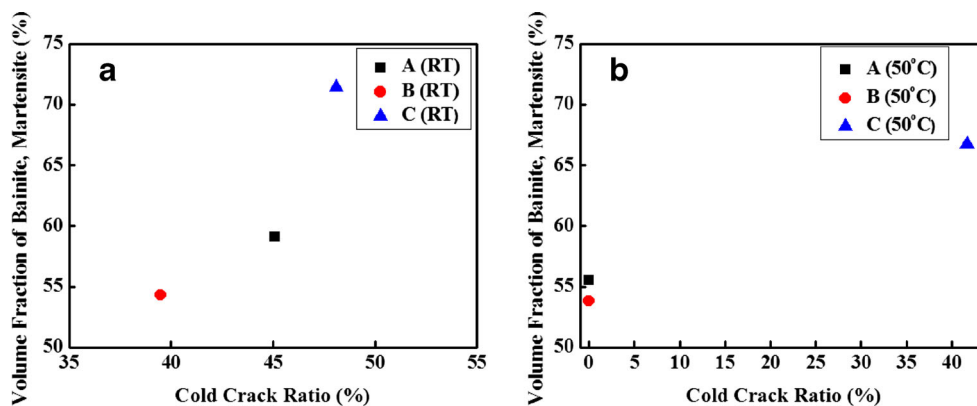


3.3 Effect of microstructure and localised Mn segregation on the cold crack ratio

Figure 5 shows the cold crack ratio as a function of the volume fraction of bainite and martensite in the weld metal. The cold crack ratio increased with increasing bainite and martensite volume fractions at room temperature and with preheating at 50 °C. Various microstructures appeared in the weld metal, such as polygonal ferrite, grain boundary ferrite, acicular ferrite, bainite and martensite. Martensite is well known as the most sensitive to cold cracking, and acicular ferrite has the greatest resistance to cold cracking due to the fine interlocking features and high-angle boundaries in the microstructure [30–32]. This result also lead to the conclusion that martensite is the most susceptible microstructure to cold cracking in weld metals.

To find the relationship between the microstructure and cold cracks in the weld metal, the cross-sectional microstructure of cold cracks in the weld metal, the cross-sectional microstructure of cold cracks was analysed. Fig. 6a shows a secondary cold crack near the main cold crack measured by an EBSD IQ image. The microstructure near the secondary crack for specimen C consisted of intergranular fracture having flat crack propagation and quasi-cleavage fracture with a non-linear path of crack propagation. In the case of intergranular fracture, as indicated in the left side of Fig. 6a, the crack indicated a sharp propagation along the grain boundary of fine lath bainite and martensite without plastic deformation. However, the central and right side of Fig. 6a showed a quasi-cleavage fracture,

Fig. 5 Cold crack ratio as a function of bainite and martensite volume fraction in the weld metal at **a** room temperature and **b** preheat temperature of 50 °C



which was occupied with a large-volume fraction of acicular ferrites as compared with the intergranular fracture region. The microstructural phases consisting of intergranular and quasi-cleavage fracture regions were identified and quantified in Fig. 6b. The intergranular fracture proceeded to the region occupied by large-volume fractions of bainite and martensite, and the quasi-cleavage fracture originated in the area having a large-volume fraction of acicular ferrite. Intergranular fracture composed of bainite and martensite showed low resistance to cold cracking. On the other hand, quasi-cleavage fracture, including the large-volume fraction of acicular ferrite, had a large resistance to cold cracking. The cold crack fractographs revealed that bainite and martensite played a role in aiding the propagation of cold cracks more so than acicular ferrite.

Figure 7 shows the back-scattered electron (BSE) image and Mn mapping near the secondary cold crack in the same area measured for Fig. 6. The weld metal showed an inhomogeneous microstructure, i.e. the region of large-volume

fraction of martensite and that of large amount of acicular ferrite. To find the cause of the inhomogeneous microstructure, EPMA analysis was conducted near the secondary cold crack. Micro-segregation of Mn was observed in the weld metal, and the region of intergranular fracture was coincident with that of high Mn content. Additionally, the quasi-cleavage area matched with the region of low Mn content, as indicated in Fig. 7b. Inhomogeneous microstructures and Mn segregation were present in all specimens A to C. Inhomogeneous microstructure in the weld metal can be successfully explained by localised Mn segregation. Furthermore, the heterogeneity contributed to the fracture type, such as intergranular and quasi-cleavage fracture, as shown in Fig. 6.

Mn is the alloying element used to increase the hardenability in steels, and an increase in Mn content promotes phase transformation to martensite[33]. During the transformation from austenite to martensite in the weldment, volume expansions occur and tensile stresses are generated in

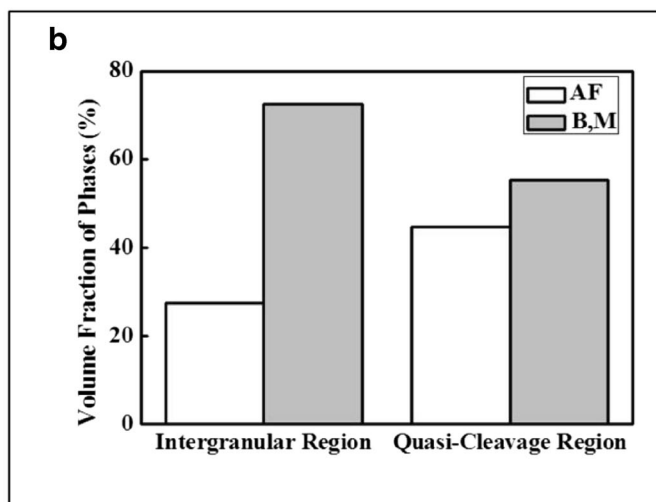
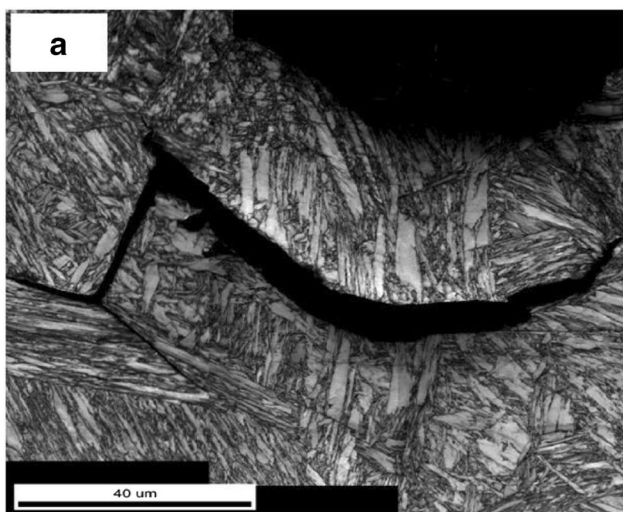


Fig. 6 Microstructure near the secondary cold crack for specimen C: **a** electron back-scatter diffraction (EBSD) IQ image of the weld metal and **b** the volume fraction of phases in the region of intergranular fracture and quasi-cleavage fracture

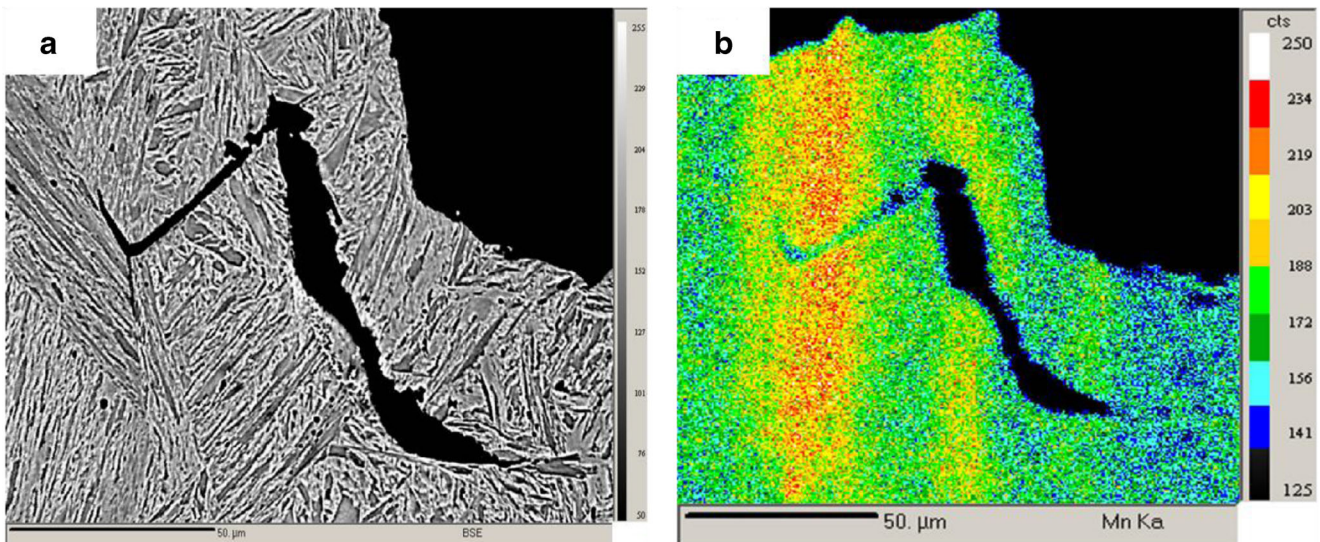


Fig. 7 EPMA analysis near the secondary cold crack in specimen C: **a** BSE image and **b** Mn mapping

the weldment [34, 35]. The tensile residual stress is one of the contributing factors in the promotion of cold cracking; therefore, large amounts of martensite transformation can also induce cold cracking. Microstructural inhomogeneity was coincident with localised Mn segregation (Fig. 7), and furthermore, with the fracture type (Fig. 6). Localised Mn segregation in FCA welding has been reported previously [36]. FCA-weld wires are produced by the metallic alloying of powders mixed with flux. As there was sufficient cooling time post-welding, the alloying elements in the FCA welding wire were completely melted and diluted with the base metal. Therefore, the chemical composition is uniform in the weld metal when the cooling time is slow. However, the alloying powders in the FCA wire can be segregated locally when the melted alloying powders are solidified without a complete dilution. Seo et al. reported that the low heat input during FCA welding increased the cooling rate and rapidly solidified the weld pool without complete dilution [37]. In this study, localised Mn segregation in the weld metal occurred because of the low heat input, 0.7 kJ/mm, applied to the Y-groove cold crack test.

3.4 The cause of cold cracking in specimen C with preheating temperature 50 °C

For a preheating temperature of 50 °C, only specimen C showed cold cracking in the weld metal, as indicated in Fig. 3. Specimen C had the largest C_{eq} and volume fraction of bainite and martensite. Figure 8 shows the volume expansion of each specimen measured by dilatometry when the specimen cooled from austenite to martensite. Specimens A to C had volume expansion ratios of 2.0, 2.1 and 2.6 %, respectively. In particular, specimen C, having the largest C_{eq} , showed the largest volume expansion ratio of 2.6 %, meaning that the largest tensile stresses could exist in weld metal C. Therefore, weld metal C has the largest probability of producing cold cracking. The reason for the largest volume expansion ratio in specimen C is associated with the many alloying elements added in the FCA wire. A previous study reported that the addition of alloying elements increased the volume expansion of martensite [38]. Therefore, specimen C, having the largest volume fraction of martensite, could promote the largest tensile stress and the cold cracking in the weld metal.

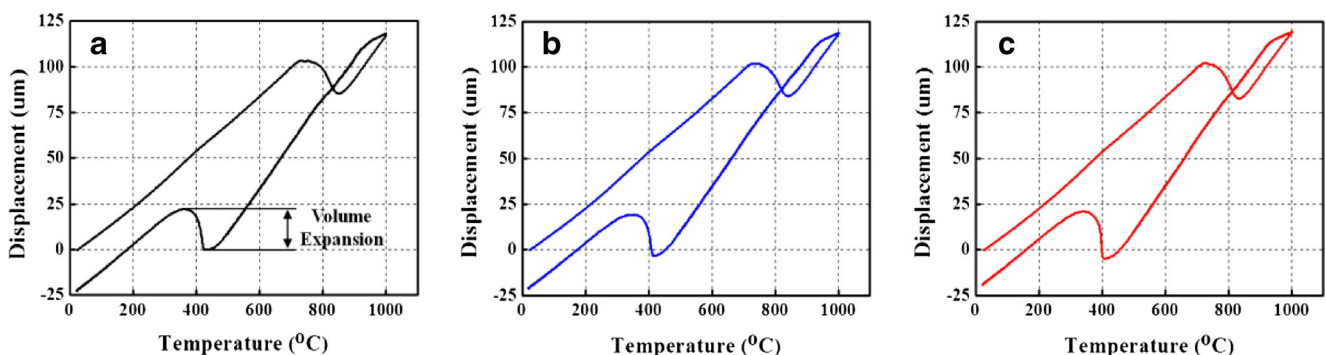


Fig. 8 Dilatometer analysis of the weld metal **a** specimen A, **b** specimen B and **c** specimen C

4 Conclusions

This study investigated the microstructural behaviour of flux-cored arc (FCA)-weld metal as a function of the welding wire composition and preheating temperature, therefore determining the relationship between the martensite volume fraction and cold crack ratio.

1. The microstructure of Y-groove weld metals consisted of acicular ferrite, bainite and martensite. At room temperature, cold cracks appeared for all weld metals A to C. As the preheating temperature increased to 50 °C, cold cracking occurred only for specimen C, having the largest carbon equivalent (Ceq). Above a preheating temperature of 100 °C, cold cracking disappeared for all weld metals. Specimen C showed the largest amount of bainite and martensite as compared with specimens A and B.

2. At room temperature, cold crack fractographs primarily exhibited intragranular fractures. As the preheating temperature increased to 50 °C, quasi-cleavage fractures appeared with a loss of intragranular fractures.

3. Intergranular fractures proceeded along the grain boundary near the region having large amounts of bainite and martensite. Quasi-cleavage fractures originated in grains having a larger volume fraction of acicular ferrite.

4. Localised Mn segregation was caused by low heat input, 0.7 kJ/mm, and led to an inhomogeneous microstructure in the weld metal. Intergranular fracture originated in areas having a large Mn segregation because of the large-volume expansion ratio. In contrast, areas of low Mn segregation produced quasi-cleavage fracture with large amounts of acicular ferrite because a small tensile stress was applied due to the low volume expansion ratio.

5. Specimen C, with the largest Ceq, presented the largest volume fraction of martensite and the highest volume expansion ratio, therefore inducing cold cracking for a preheating temperature of 50 °C.

Acknowledgments This work was financially supported by the Ministry of Trade, Industry and Energy (no. 10035163) and the National Research Foundation of Korea (NRF) grant funded by the Korea government (MSIP) through GCRC-SOP (no. 2011-0030013).

References

- Kitada T, Fukuda K (1986) Nippon Kokan Technical Report. 47: 58–64
- Fisher JW, Dexter RJ (1994) High-performance steels for America's bridges. *Weld J* 73(1):35–43
- Parmar RS (ed) (1999) *Welding processes and technology*. Khanna Publishers, New Delhi, pp 53–61
- Davidson JL (1998) Advances in hydrogen management: the science based design of Low hydrogen consumables for the future. *Australas Weld J* 43(3):33–39
- Kuebler R, Pitrun M, Pitrun I (2000) The effect of welding parameters and hydrogen levels on the weldability of high strength Q&T steel welded with FCAW consumables. *Australas Weld J* 45(1):38–47
- Kou S (1987) *Welding metallurgy*. John Wiley and Sons, New York
- Easterling K (1983) *Introduction to the physical metallurgy of welding*. Butterworths & Co Ltd
- Wildash C, Cochrane RC, Gee R, Widgery DJ (1998) Microstructural factors affecting hydrogen induced cold cracking in high strength steel weld metals. *Trends in Welding Research*, Georgia, USA
- Lee HW, Kang SW, Um DS (1998) A study on transverse weld crack in thick steel plate with FCAW process. *Weld J* 77(12):503–510
- White D, Pollad G, Gee R (1992) The effect of welding parameters on diffusible hydrogen levels in cored wire welding. *Weld Met Fabr* 60(6):209–216
- Dixon B, Hakansson K (1995) Effects of welding parameters on weld zone toughness and hardness in 600 MPa steel. *Weld J* 74(4): 122–132
- Kiefer JH (1996) Effects of moisture contamination and welding parameters on diffusible hydrogen. *Weld J* 75(5):155–161
- Harwig DD, Longenecker DP, Cruz JH (1999) Effects of welding parameters and electrode atmospheric exposure on the diffusible hydrogen content of gas shielded flux cored welding. *Weld J* 78(9):314–321
- Pitrun M, Davidson JL, Kenny CJ, Wittke PJ, Cornish N (2001) Factors affecting the hydrogen content of weld metal deposited by flux cored arc welding consumables. *Australas Weld J* 46(1):33–38
- Pitrun M, Nolan D (2006) Susceptibility of low strength rutile flux-cored weld metal to hydrogen assisted cold cracking. *Weld World* 50(5/6):24–37
- Enzinger N, Cerjak H (2007) Characterization of cracks in high strength steel weldments. *Weld World* 51(11/12):29–33
- Sierdzinski MS, Ferree SE (1998) New flux core wires control diffusible hydrogen levels. *Weld J* 77(2):45–48
- Marchenko AE (1995) Development of technology for producing low-hydrogen electrode. *Weld Int* 9(1):51–55
- Matsushida M, Liu S (2000) Hydrogen control in steel weld metal by means of fluoride addition in welding flux. *Weld J* 79(10):295–303
- Hart PHM (1986) Resistance to hydrogen cracking in steel weld metal. *Weld J* 65(1):14–22
- Lee HW (2007) Weld metal hydrogen-assisted cracking in thick steel plate weldments. *Mater Sci Eng A* 445–446:328–335
- Seo JS, Kim HJ, Ryoo HS (2008) Effect of grain boundary ferrite on susceptibility to cold cracking in high-strength weld metal. *Met Mater Int* 14(4):515–522
- Kim JH, Kim JS, Ryoo HS, Kim KH, Huh MY (2008) Effect of weld metal microstructures on cold crack susceptibility of FCAW weld metal. *Met Mater Int* 14(2):239–245
- IIW/IIS DOC. 452-74. (1974) *Welding in the World* 12(3/4):65–69
- AWS A 4.3. (1993) American Welding Society
- ISO 17642-2 (2005) *Destructive tests on welds in metallic materials—cold cracking tests for weldments—arc welding processes part 2. Self-restraint tests*
- Kannengiesser T, Boellinghaus T (2013) Cold cracking tests—an overview of present technologies and applications. *Weld World* 57: 3–37
- Seo JS, Kim HS, Ryoo HS (2008) Microstructural parameter controlling weld metal cold cracking. *JAMME* 27(2):199–202
- Lee JH, Kim SH, Yoon BH, Kim HT, Kil SC, Lee CH (2011) Microstructural characteristics of 800 MPa grade high strength steel weld metals. *J KWJS* 29(1):65–73 (in Korean)
- Garland JR, Kirkwood PR (1975) Toward improved submerged arc weld metals. *Metal Constr Part 1* 7(5):275–283

31. Garland JR, Kirkwood PR (1975) Toward improved submerged arc weld metals. *Metal Constr Part 2* 7(6):320–330
32. Lee MJ, Kang NH (2014) The effects of microstructure on cold crack in high-strength weld metals. *J KWJS* 32(1):22–27 (in Korean)
33. Bhadeshia H and Honeycombe R (2011) *Steels: microstructure and properties*. Butterworth-Heinemann
34. Wang W, Huo L, Zhang Y, Wang D, Jing H (2002) New developed welding electrode for improving the fatigue strength of welded joints. *J Mater Sci Technol* 18:527–531
35. Murata H, Kato N, Tamura H (1993) Effect of transformation on residual stress in welding. *Yosetsu Gakkai Ronbunshu/Q J Japn Weld Soc* 11:545–50
36. Pargeter RJ (1992) Effects of arc energy, plate thickness and preheat on C-Mn steel weld metal hydrogen cracking. TWI report No. 461/1992, TWI, Abington Cambridge, UK
37. Seo JS, Kim JH, Kim HJ, Ryoo HS (2007) Characteristics of cold cracks in FCA weld metal. *J KWJS* 25(4):242–346 (in Korean)
38. Shibata A, Yonezawa H, Yabuuchi K, Morito S, Furuhashi T, Makia T (2006) Relation between martensite morphology and volume change accompanying fcc to bcc martensitic transformation in Fe–Ni–Co alloys. *Mater Sci Eng A* 438–440:241–245